Bohayra Mortazavi Markus Pötschke, Gianaurelio Cuniberti

Multiscale modeling of thermal conductivity of polycrystalline graphene sheets

Erstveröffentlichung in / First published in:
Nanoscale. 2014, 6(6), S. 3344–3352 [Zugriff am: 04.11.2019]. Royal Society of Chemistry. ISSN 2040-3372.

DOI: https://doi.org/10.1039/c3nr06388g

Nanoscale

PAPER

View Article Online
View Journal | View Issue

Cite this: *Nanoscale*, 2014, **6**, 3344

Multiscale modeling of thermal conductivity of polycrystalline graphene sheets

Bohayra Mortazavi,†*[ab] Markus Pötschke†[ab] and Gianaurelio Cuniberti[abcd]

Received 2nd December 2013
Accepted 3rd January 2014

DOI: 10.1039/c3nr06388g

www.rsc.org/nanoscale

We developed a multiscale approach to explore the effective thermal conductivity of polycrystalline graphene sheets. By performing equilibrium molecular dynamics (EMD) simulations, the grain size effect on the thermal conductivity of ultra-fine grained polycrystalline graphene sheets is investigated. Our results reveal that the ultra-fine grained graphene structures have thermal conductivity one order of magnitude smaller than that of pristine graphene. Based on the information provided by the EMD simulations, we constructed finite element models of polycrystalline graphene sheets to probe the thermal conductivity of samples with larger grain sizes. Using the developed multiscale approach, we also investigated the effects of grain size distribution and thermal conductivity of grains on the effective thermal conductivity of polycrystalline graphene. The proposed multiscale approach on the basis of molecular dynamics and finite element methods could be used to evaluate the effective thermal conductivity of polycrystalline graphene and other 2D structures.

1. Introduction

Graphene,[1] a single layer form of carbon atoms, is an exceptional material because of its unique properties.[2–4] Graphene is a highly attractive material due to its exceptionally high thermal conductivity,[5] mechanical[6] and electrical properties.[7] The unique combination of high thermal, mechanical and electrical properties renders graphene as an extraordinary material for a wide variety of applications from nanoelectronics to the aerospace industry. It should be noted that the reported good thermal, mechanical and electrical properties of graphene belong to samples of defect-free, single crystal and single-layer graphene. Therefore, the properties of graphene like all other known materials could be affected by the existence of defects in the crystal lattice. Graphene, being a highly stable material, does not allow the formation of any detectable concentration of defects at temperatures below its melting point.[8] It has been reported[8] that the lattice defects in graphene are formed primarily during the fabrication of graphene sheets. The first challenge in regulating the defect concentration of graphene sheets therefore lies in controlling the fabrication process. Moreover, for practical applications of graphene, it is of crucial importance to develop the fabrication processes such that they can produce large-scale graphene sheets. Among all the developed approaches for the fabrication of graphene sheets, the chemical vapor deposition (CVD) technique is the only way to produce industry-scale graphene sheets.[9] Crystal growth during the CVD method leads to the formation of polycrystalline graphene structures rather than monocrystalline structures. In a polycrystalline graphene sheet, at places where the grains meet, grain boundaries form, which consist of topological defects and are considered as dislocation cores, as opposed to within the grains. As the grain size decreases, the number of carbon atoms along the grain boundaries increases and accordingly the defect concentration in the structure increases. It is therefore expected that the grain boundaries in polycrystalline graphene sheets grown by the CVD technique may not only decrease the electrical and thermal conductivity of graphene but also substantially affect the structural stability of graphene under mechanical loading.[10] A fundamental understanding of grain boundary effects on the mechanical, thermal and electrical properties of graphene is therefore of crucial importance for the future applications of graphene.

Using first principles calculations, it has been reported that the grain boundaries in graphene comprise a series of pentagon/heptagon pairs.[11,12] These observations promoted a number of investigations on the heat flow across the graphene grain boundaries using molecular dynamics (MD) simulations.[13,14] In all of the MD models developed in these studies, periodic boundary conditions were applied along the graphene width, which implies that the results correspond to infinite grain boundaries. Therefore, it is difficult to correlate the reported results with the bulk polycrystalline graphene sheets.

[a]*Institute for Materials Science and Max Bergman Center of Biomaterials, TU Dresden, 01062 Dresden, Germany. E-mail: bohayra.mortazavi@nano.tu-dresden.de; Fax: +49-351-46331422; Tel: +49-176-68195567*

[b]*Dresden Center for Computational Materials Science, TU Dresden, 01062 Dresden, Germany*

[c]*Center for Advancing Electronics Dresden, TU Dresden, 01062 Dresden, Germany*

[d]*Center for Transport and Devices of Emergent Materials, TU Dresden, 01062 Dresden, Germany*

† These authors contributed equally.

Recently, Kotakoski and Meyer[15] proposed a methodology for the construction of polycrystalline graphene sheets. The constructed molecular models were then used to study the mechanical[15] and charge transport[16] response of polycrystalline graphene.

The objective of this study is to provide a new viewpoint concerning the thermal conductivity of polycrystalline graphene sheets using a combination of atomistic and continuum approaches. To this aim, MD simulations were performed for the evaluation of the thermal conductivity of ultra-fine grained graphene sheets. We used a similar methodology to that explained in ref. 15 for the construction of realistic molecular models of relatively large polycrystalline graphene sheets with equivalent grain sizes ranging from 1 nm to 5 nm consisting of 25 up to 400 grains. Subsequently, the equilibrium molecular dynamics (EMD) approach was employed to study the grain size effect on the thermal conductivity of ultra-fine grained graphene samples. As expected, the EMD results demonstrated that decreasing the grain size decreases the thermal conductivity due to phonon scattering at the grain boundaries. The EMD results reveal that the ultra-fine grained graphene structures have thermal conductivity one order of magnitude smaller than that of pristine graphene. The high computational costs of MD simulations impose strict limitations for the modeling of larger systems. While MD modeling is a powerful tool for studying the material's response at an atomic level, it is computationally unfeasible in the study of materials with macroscopic sizes, such as polycrystalline graphene sheets with microscale grain sizes. Thus, in addition to the atomistic modeling by the MD method, macroscopic polycrystalline graphene models were constructed using the finite element approach. In the finite element models, all the grain boundaries were assumed to exhibit an effective contact conductance. This effective thermal conductance was acquired by fitting the finite element results to the EMD results for ultra-fine grained structures. By performing the finite element calculations for the systems with larger grain sizes, close agreement between the finite element results and the EMD extrapolated curve was observed. We also employed the finite element approach to investigate the effect of grain size distributions on the effective thermal conductivity of polycrystalline graphene sheets. The proposed multiscale approach in this study could be used efficiently to evaluate the thermal conductivity of polycrystalline graphene and other 2D structures.

2. Molecular dynamics modeling

In this study, classical molecular dynamics simulations were carried out in order to evaluate the thermal conductivity of ultra-fine grained polycrystalline graphene sheets at room temperature (300 K). Molecular dynamics calculations in this study were performed using LAMMPS (Large-scale Atomic/Molecular Massively Parallel Simulator),[17] which is a free and open-source package. Second-generation reactive empirical bond order (REBO) potential[18] was used to model the covalent interactions of carbon atoms. In all the molecular dynamics calculations in this study, periodic boundary conditions were applied in planar directions and simulation time increment was fixed at 1 fs. MD simulations were performed in the microcanonical ensembles starting from initial configurations and then equilibrated at 300 K. Moreover, the Nosé–Hoover barostat and thermostat method was used to relax the structures at zero stress. Once the system was free of residual stresses, the structures were further equilibrated at room temperature using Berendsen thermostat. At this stage, the system is at equilibrium conditions and the energy of the system is conserved by performing the constant energy (NVE) calculations. The equilibrium molecular dynamics (EMD) method was used to evaluate the thermal conductivity of graphene. The EMD method relies on relating the ensemble average of the heat current autocorrelation function (HCACF) to the thermal conductivity k, *via* the Green–Kubo expression:

$$k_\alpha = \frac{1}{VK_B T^2}\int_0^\infty \langle J_\alpha(t)J_\alpha(0)\rangle \mathrm{d}t \quad (1)$$

where α denotes the three Cartesian coordinates, K_B is the Boltzmann's constant, V and T are the volume and temperature of the system respectively. The auto-correlation functions of the heat current $\langle J_\alpha(t)J_\alpha(0)\rangle$ can be calculated using the heat current $\overrightarrow{J(t)}$ as expressed by:[17]

$$\overrightarrow{J(t)} = \sum_i \left(e_i \overrightarrow{v_i} + \frac{1}{2}\sum_{i<j}\left(\overrightarrow{f_{ij}}\cdot\left(\overrightarrow{v_i} + \overrightarrow{v_j}\right)\right)\overrightarrow{r_{ij}}\right) \quad (2)$$

here, e_i and v_i are respectively the total energy and velocities of atom i, f_{ij} and r_{ij} are respectively the interatomic force and position vector between atoms i and j. By performing the constant energy simulations, the heat current values along planar directions were recorded in order to calculate the HCACF. Using eqn (1), the thermal conductivity of graphene structures is obtained by averaging the HCACFs along the planar directions and for several independent simulations.

During the fabrication of graphene sheets using the CVD method, the growth of graphene along arbitrary crystal orientations is initiated at several nucleation sites simultaneously. We developed a program in order to simulate such a growth mechanism by creating a preselected number of randomly placed nucleation sites on a plane with predefined dimensions. The initial nucleation sites were randomly and uniformly distributed in the plane. By assuming a square geometry for an equivalent average grain in a polycrystalline graphene sheet, the grain size in this study is defined by $\sqrt{\frac{L^2}{N}}$, where L is the side length and N is the number of grains in the plane. In this way, the equivalent average grain size for a plane with 20 nm length and 100 grains would be 2 nm. Each nucleation site was subsequently assigned a random angle between 0° and 90° so as to define the grain growth orientation. The growth of nucleation sites were then performed using an iterative process in which any of the missing neighbors of a boundary atom can appear with the same probability. Further growth of a grain from a boundary atom is terminated when it meets with another atom from the neighboring grain with a distance

of below 0.1 nm. The growth of polycrystalline graphene is completed when all the grains meet with their neighbors and there is no possibility for any atom to be added in a lattice. In order to remove the effects of edge atoms on the reported effective properties, the constructed models were developed by taking into account the periodicity criterion. This means that if one puts these samples side by side together no mismatch in the lattices should be observed. This is to ensure that the reported properties are from graphene sheets and not from graphene nanoribbons. After creating initial positions for carbon atoms, MD calculations were used to form the grain boundaries in the polycrystalline graphene sheets. The initial structures were equilibrated at room temperature (300 K) for 50 ps using the Nosé–Hoover thermostat method (NVT). Then, the structures were uniformly heated to 3000 K, below the melting point of graphene using the NVT method for 50 ps. At this stage, the temperature of the systems was kept at 3000 K using the NVT method for 50 ps. The high mobility of carbon atoms at 3000 K allows rearrangement of their positions until the minimum energy state is achieved. Next, the samples were cooled from 3000 K to room temperature for 50 ps. The structures were then equilibrated at 300 K for another 50 ps using the NVT method. To ensure the accurate equilibrium state of the structures, the systems were finally relaxed to zero stresses at room temperature using the Nosé–Hoover barostat and thermostat method (NPT) for 10 ps. At this stage, the structure is accurately prepared for the evaluation of thermal conductivity.

3. Atomistic results

Fig. 1 depicts two samples of ultra-fine grained graphene sheets constructed with an average grain size of 2 nm with 100 grains and an average grain size of 5 nm with 25 grains. In the constructed samples, the grain boundaries and grain boundary junctions are formed similarly to the samples reported in the work by Kotakoski and Meyer.[15] The side views in Fig. 1 illustrates that by decreasing the grain size, the defective zones spread more along the graphene sheet and cause the structure to undergo considerable deformation and deflection. Moreover, different types of grain boundaries could be observed which is naturally linked to the misorientation angle between two adjacent grains. In this way, where the misorientation angle between two neighboring grains is small, the grain boundaries are free of defects and one could not easily distinguish the initial grains.

The constructed polycrystalline graphene structures were used to study the grain size effect on the thermal conductivity of graphene. In this work, for each grain size, the thermal conductivity was calculated for two different samples with different grain configurations. Moreover, for each sample, the calculations were performed for six different simulations with uncorrelated initial conditions. The results for each simulation were averaged along the planar directions (x and y directions). In Fig. 2, the calculated thermal conductivity of pristine and ultra-fine grained graphene structures as a function of correlation time is shown. The MD results reveal that at the

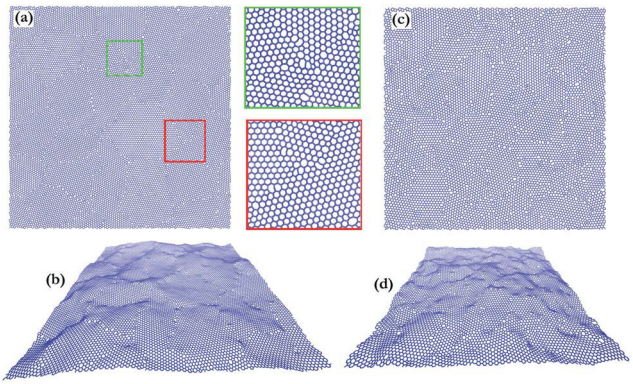

Fig. 1 Molecular models of ultra-fine grained graphene sheets. (a) Top and (b) side views of periodic 25 nm × 25 nm polycrystalline graphene with an average grain size of 5 nm consisting of 25 grains. (c) Top and (d) side views of periodic 20 nm × 20 nm polycrystalline graphene with an average grain size of 2 nm consisting of 100 grains.

correlation time of 10 ps, the thermal conductivity for pristine graphene is well-converged. By decreasing the grain size, the thermal conductivity converges at lower correlation times. Moreover, distinct differences between the thermal conductivity of pristine and ultra-fine grained graphene samples can be observed. To ensure the size independency of the reported results, the calculations were performed up to around 25 000 atoms for pristine graphene. Using eqn (1), the thermal conductivity of pristine graphene was calculated to be 280 ± 15 W m^{-1} K^{-1}, which is one order of magnitude below the experimentally measured thermal conductivity of single-layer graphene.[5] The REBO potential has been widely used for the modeling of thermal conductivity of graphene structures.[19–23] Using the non-equilibrium molecular dynamics (NEMD) and REBO potential, Thomas *et al.*[19] reported that the thermal conductivity of bulk graphene with a length of 600 nm converges at 350 W m^{-1} K^{-1}. However, it is worthy to note that in other NEMD studies with REBO potential, the thermal conductivity of graphene was reported to be within the range

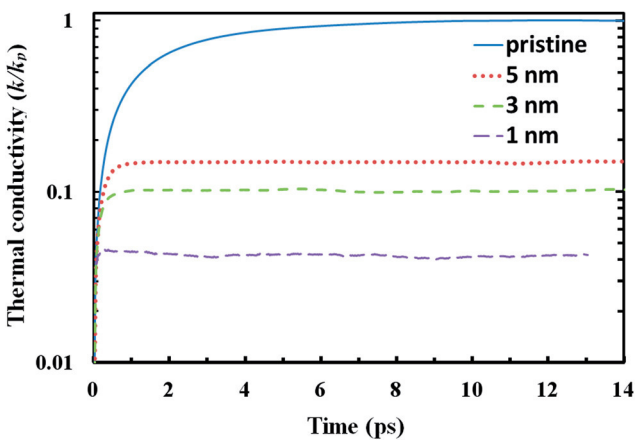

Fig. 2 Normalized thermal conductivity of ultra-fine grained graphene sheets with respect to the pristine graphene thermal conductivity, k_p.

of 1000 to 2000 W m^{-1} K^{-1}.[21–23] It should be emphasized that our aim is a comparative study of the grain size effect on the thermal conductivity of graphene and not to reproduce an accurate thermal conductivity of defect-free graphene. Accordingly, in this study, we report the normalized thermal conductivity of polycrystalline structures with respect to the thermal conductivity of pristine graphene. We note that the optimized Tersoff potential developed by Lindsay and Broido[24] yields more accurate results for thermal conductivity of pristine graphene. Using the NEMD simulations along with the optimized Tersoff potential, we calculated a thermal conductivity of 3000 W m^{-1} K^{-1} for pristine graphene[25,26] in close agreement with Boltzmann transport calculations.[24] However, a recent EMD study using the optimized Tersoff potential reports a lower thermal conductivity of around 1000 W m^{-1} K^{-1} for pristine graphene.[27] Importantly, we found that the optimized Tersoff potential[24] could not be employed neither in the construction of polycrystalline samples nor in the evaluation of thermal conductivity. This is mainly due to the limited reactivity of Tersoff potentials[28,29] which does not allow the formation of complex grain boundaries. Moreover, for the constructed polycrystalline graphene samples, we found that the optimized Tersoff potential could not accurately control the temperature fluctuations at room temperature.

The normalized thermal conductivities of ultra-fine grained graphene sheets with respect to the pristine graphene thermal conductivity are illustrated in Fig. 3. As expected, the thermal conductivity of graphene decreases sharply as the grain size decreases. Our results suggest that the ultra-fine grained graphene structures have thermal conductivity one order of magnitude lower in comparison with the defect-free graphene. Using the obtained results for ultra-fine grained graphene, we could estimate the thermal conductivity of polycrystalline graphene samples. We note that the effective conductivity of a series of line conductors with equal length and connected with point conductors is dependent on the conductor's length through a first order rational curve (see Appendix A). Therefore, we fit a first order rational curve (as presented in Fig. 3 with a dashed line) with a very good accuracy to extrapolate the EMD results in order to explore the thermal conductivity of polycrystalline graphene sheets having larger grain sizes which are very difficult to study by atomistic based approaches. Interestingly, the extrapolated results suggest that for an average grain size of 600 nm, which represents the mean free path of graphene at room temperature,[30] the thermal conductivity of polycrystalline graphene would be only 2% less than that of pristine graphene.

To relatively examine the mechanism responsible for this reduction of thermal conductivity in polycrystalline graphene samples, we calculate the carbon atom phonon density of states (PDOS). The PDOS was computed by calculating the Fourier transformation of carbon atom velocity autocorrelation functions by the following relationship:

$$\text{PDOS}\ (\omega) = \int < v(t)v(0) > e^{-i\omega t}\mathrm{d}t \qquad (3)$$

where ω is the frequency and v is the velocity of carbon atoms. In Fig. 4, the calculated PDOS curves for carbon atoms in pristine graphene and those along the grain boundary and grain boundary junction are plotted. We note that the PDOS of carbon atoms inside the grains are similar to those of pristine graphene with characteristic peaks occurring at the same frequencies. For pristine graphene a main peak at 50 THz exists, which is characteristic of the two-dimensional graphene sheet phonon spectrum. As the first finding, we could observe that PDOS curves for carbon atoms along grain boundary and grain boundary junctions appear to be very similar. In these cases, the phonon scattering cause considerable damping of the main peak around 50 THz. On the other side, the PDOS calculation reveals that the damping of low frequency phonons along the grain boundaries is insignificant. Since the dominant heat carriers in graphene are low frequency acoustic phonons, the PDOS results suggest high thermal conductance of grain boundaries.

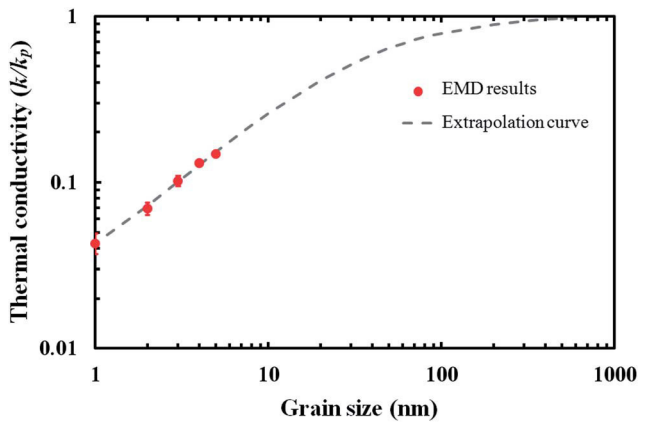

Fig. 3 Normalized thermal conductivity of polycrystalline graphene sheets as a function of grain size. The dot points are the EMD results for ultra-fine grained graphene and the dashed line is the fitted curve by the use of EMD results to predict the thermal conductivity of polycrystalline graphene structures with larger grain sizes.

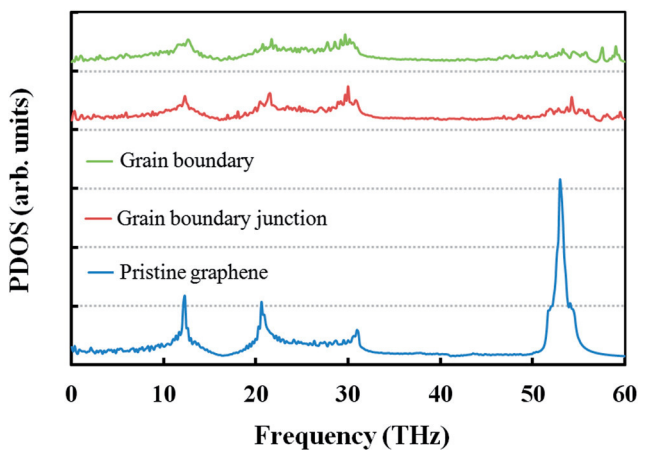

Fig. 4 Calculated phonon density of states (PDOS) for carbon atoms in pristine graphene and carbon atoms in grain boundary and grain boundary junctions.

4. Multiscale results and discussion

To provide a better viewpoint concerning the effective thermal conductivity of polycrystalline graphene structures with larger grain sizes, we used the finite element approach. The main advantage of the finite element in comparison with atomistic modeling is that one could study the systems at the macroscopic scale and over long periods while the atomistic modeling is commonly limited to studying very small sample sizes at the nanoscale and for extremely short times on the order of nanoseconds. However, in the finite element modeling of macroscopic samples, the atomistic effects are neglected. Accordingly, the combination of finite element and atomistic simulations is a promising approach to pass the limits associated with each of the methods. From this point of view, one could use atomistic simulations to provide the information to enrich the finite element modeling in order to study the material properties at the macroscopic scale.[31] Motivated by this idea, we aimed to develop a methodology on the basis of finite element and molecular dynamics to systematically study the thermal conductivity of polycrystalline graphene sheets. In the finite element modeling in this study, in a similar way to our MD modeling, we uniformly distributed 1000 points in square planes with predefined dimensions. Each point is then considered to be the center of a grain in the desired microstructure. Based on the distributed points, we constructed Voronoi cells with mirror symmetry at all edges. We used COMSOL package for the extensive finite element simulations in this study. Samples of constructed polycrystalline graphene sheets are shown in Fig. 5. For the evaluation of thermal conductivity, we used the one dimensional form of the Fourier law:

$$k_{\text{eff}} = q\frac{L}{\Delta T} \tag{4}$$

here, k_{eff} is the effective thermal conductivity of the structure and q is the heat flux. In this approach, we applied a temperature difference (ΔT) of 0.2 K along two opposite edges and the resulting heat flux (q) over the entire sample was averaged to calculate the effective thermal conductivity. The thermal contact interactions between adjacent grains are introduced by using contact elements with an effective grain boundary conductance. In this study, we assume that the grains have the same thermal conductivity as that of pristine graphene and all the grain boundaries exhibit a common effective contact conductance. To evaluate this effective contact conductance, we fit the finite element results to the five data points provided by the EMD approach. By performing the finite element calculations, the effective contact conductance of polycrystalline graphene samples was measured with respect to the pristine thermal conductivity (k_{pristine}) to be: $k_{\text{pristine}}/(30.0\text{ nm})$. If we assume the thermal conductivity of single layer graphene to be 4000 W m^{-1} K^{-1} as reported in ref. 5, the effective grain boundary conductance would be around 133 GW m^{-2} K^{-1}. Using the NEMD approach, Bagri *et al.*[13] reported grain boundary conductance of 15 GW m^{-2} K^{-1} to 45 GW m^{-2} K^{-1} for three different misorientation angles. This discrepancy with MD results could be explained by several reasons. First, the calculated grain boundary conductance is an averaged and

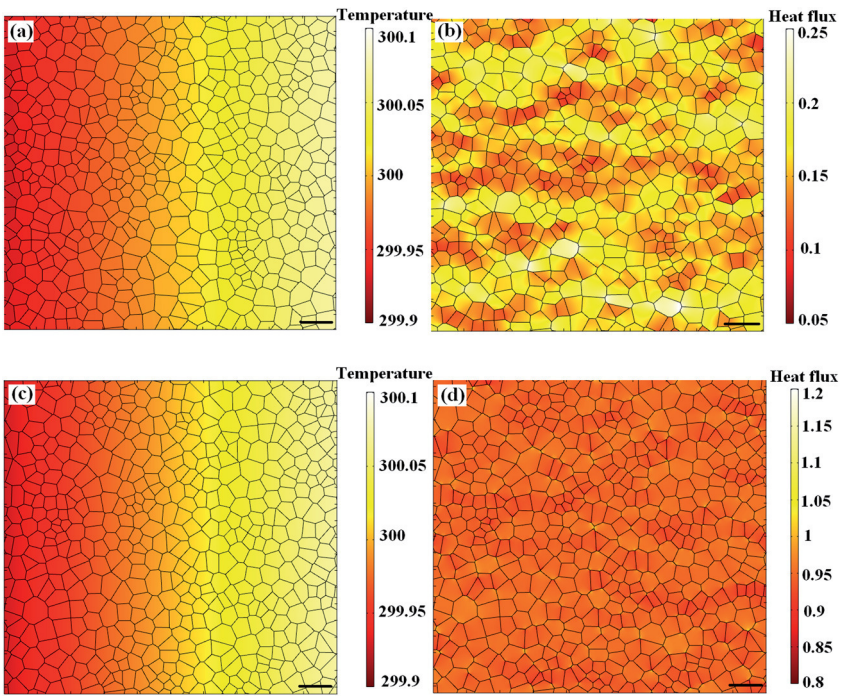

Fig. 5 Samples of constructed finite element models for the evaluation of thermal conductivity of polycrystalline graphene structures. (a) Temperature and (b) heat flux distribution of a polycrystalline graphene sheet with an average grain size of 5 nm (the scale bar is 10 nm). (c) Temperature and (d) heat flux distribution of a polycrystalline graphene sheet with an average grain size of 500 nm (the scale bar is 1000 nm).

effective value, which is applied to all grain boundaries even along those with small misorientation angles. For small misorientation angles for two neighboring grains, the formed grain boundary is defect-free, which consequently means that the thermal conductance of the grain boundary is infinite. As shown in Fig. 1a, the constructed sample consists of several defect-free grain boundaries. Secondly, the conductivity of the grain boundaries depends strongly on the wavelength of the transmitted phonons. Thus, for large samples with many grain boundaries, phonons with an unfavorable wavelength contribute only little to the total conductivity. The average conductivity of the phonons that do contribute to the effective conductivity is significantly higher if only a few grain boundaries are considered. Moreover, the work by Bagri *et al.*[13] did not show limits for grain boundary conductance values, since increasing trends were reported as the length of samples increased. On the other hand, in our approach the grain boundary conductance is linked to the prediction of the thermal conductivity of pristine graphene. We note that in the work by Bagri *et al.*,[13] the thermal conductivity of pristine graphene was reported to be 2650 W m^{-1} K^{-1}, and based on our finding the effective contact conductance would be 88 GW m^{-2} K^{-1}, which is in closer agreement with the results reported in ref. 13. We would like to remind that our finding for grain boundary conductance is on the basis of relying on the REBO potential results for the relative thermal conductivity of polycrystalline graphene with respect to that of pristine graphene. Therefore, further studies with other inter-atomic potential functions for carbon atoms are necessary to provide a more comprehensive vision.

In Fig. 5, samples of constructed finite element models for uniform grain distributions with an average grain size of 5 nm (Fig. 5a and b) and 500 nm (Fig. 5c and d) are shown. As discussed earlier, a temperature difference of 0.2 K was applied along the sample as the loading condition. Because of the applied boundary condition, the established temperature distributions throughout the entire sample are similar for the two studied cases. However, for the sample with an average grain size of 5 nm, the temperature distributions inside the grains are relatively constant and the established temperature profile for the entire sample is mainly due to the jumps at the grain boundaries. On the other side, considerable differences in the heat flux distributions throughout the samples for the two different studied grain sizes could be observed. As the first finding, the established heat flux distribution for the grain size of 5 nm is presenting a considerably inhomogeneous profile while for the larger grain size it is found to be more uniform. For the small grain size, the grain boundaries present the major contribution to the effective thermal resistance of the sample. Thus, the grains with larger length along the applied temperature difference carry the most thermal heat flux. For a larger grain size of 500 nm, the grain boundary contribution is smaller and therefore the overall heat flux distribution presents a much more uniform and homogeneous response. We note that the magnitude of heat flux values is proportional to the effective thermal conductivity of the structure. Thus, for an average grain size of 500 nm, the heat flux values are almost in one order of magnitude higher than those for the sample with an average grain size of 5 nm.

In Fig. 6, we compared the normalized effective thermal conductivity of polycrystalline graphene sheets calculated by the finite element method with the EMD results' extrapolation curve. In this study, the finite element calculations for every grain size were performed for five different microstructures with different random grain configurations and the calculated errors were smaller than the maker size in Fig. 6. The finite element approach yields considerably close results to the EMD estimations for the entire range of studied grain sizes. As mentioned previously, in our finite element modeling we assumed that the grains have the same thermal conductivity as that of the pristine graphene. To examine the error that might be raised due to this assumption, the finite element calculations were performed for the case that the thermal conductivity of grains was 10% below that of pristine graphene thermal conductivity and the obtained results are also plotted in Fig. 6. Interestingly, we found that at low grain sizes the effective thermal conductivity is negligibly affected, whereas at large grain sizes (higher than 200 nm) a reduction with the same order (around 10%) is observed. This observation is principally due to the fact that for the small grain sizes, the contact resistance between the grains plays the major role, while for grain sizes larger than 100 nm the thermal conductivity of grains is the key factor for the effective thermal conductivity. Consequently, assuming a lower thermal conductivity for the grains in the ultra-fine grained samples does not considerably affect the finite element estimations. Moreover, when the grain size is close to the mean free path of pristine graphene (600 nm as reported in ref. 30), assuming the pristine graphene thermal conductivity for the grains is justified.

Up to this stage, in our finite element modeling, we assumed that the grains exhibit uniform size distributions. It is worth mentioning that the experimentally fabricated polycrystalline

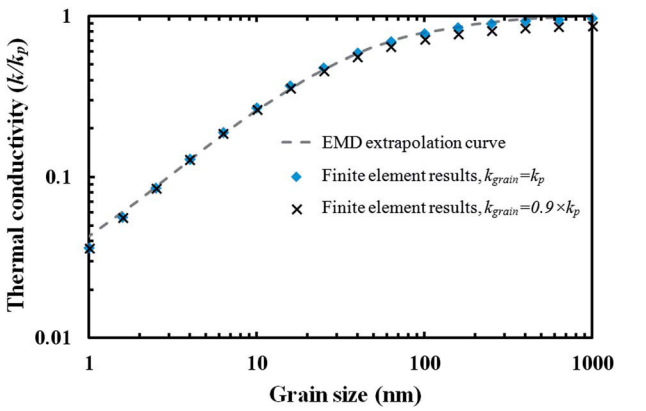

Fig. 6 Comparison of finite element results with the EMD results' extrapolation curve for the thermal conductivity of polycrystalline graphene sheets. The results are normalized with respect to the pristine graphene thermal conductivity k_p. The finite element calculations were performed for two different cases in which the grain thermal conductivity, k_{grain} is equal to or 10% below the pristine graphene thermal conductivity.

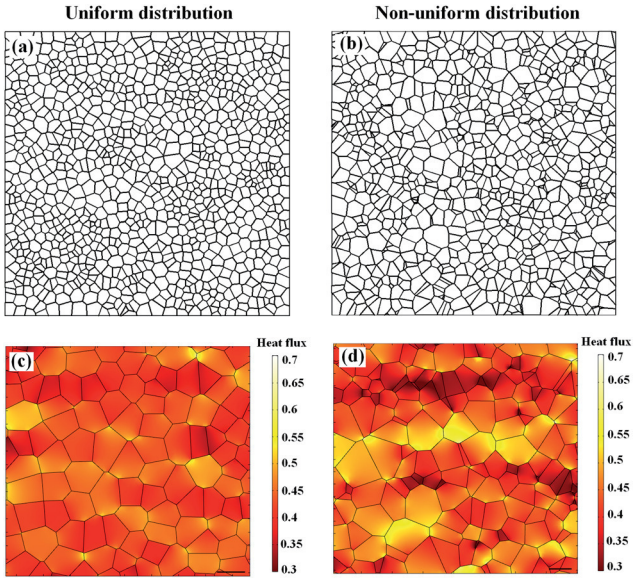

Fig. 7 Constructed finite element models of polycrystalline graphene sheets with an average grain size of 20 nm for (a) uniform and (b) non-uniform grain distribution. Established heat flux distributions for (c) uniform and (d) and non-uniform grain configurations.

graphene samples exhibit mainly non-uniform grain distribution rather than uniform configuration.[32–34] Accordingly, to examine the intensity of the grain distribution effect on the reported effective thermal conductivity, we constructed the finite element models with different grain configurations. In Fig. 7, the constructed finite element models of polycrystalline graphene sheets with an average grain size of around 20 nm for uniform and non-uniform grain configurations are illustrated. In Fig. 8, we plot the multiscale results for relative difference of thermal conductivity of polycrystalline graphene structures with non-uniform and uniform grain distributions as a function of grain size. The obtained result indicates that the relative differences between the uniform and non-uniform grain distributions sharply decrease as the grain size increases. We found that this relative difference becomes negligible for the grain sizes higher than 500 nm. To better understand the underlying mechanism for this improvement, we also plotted

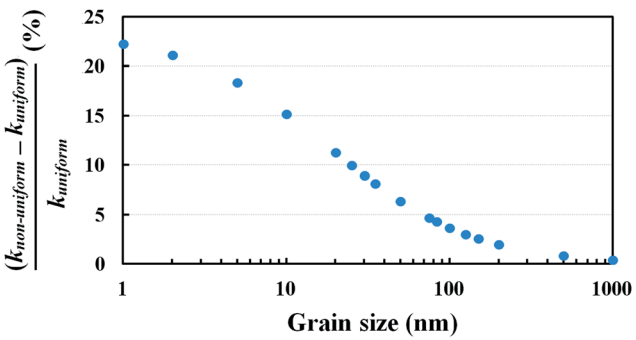

Fig. 8 Multiscale results for relative difference in the thermal conductivity of polycrystalline graphene structures with non-uniform and uniform grain distributions as a function of grain size.

the heat flux distribution throughout the two studied samples (see Fig. 7c and d). At first glance, one could observe a remarkably higher contrast in heat flux values for the sample with non-uniform grain distribution in comparison with the uniform case. As already discussed, for the ultra-fine grained structures, the contact resistance between the grains is understood to be the main factor in determining the overall effective thermal conductivity. In these cases, the larger grains transfer the major part of the heat flux. This way, by increasing the difference between the grain sizes for the samples with non-uniform grain distributions, the heat flux is carried primarily through the large grains and mainly along those large grains that are percolating together, which results in a higher effective thermal conductivity of the sample (see Fig. 7d). Accordingly, by decreasing the importance of grain boundary conductance for the polycrystalline samples with larger grain sizes, the intensity of the grain's distribution effect on the thermal conductivity would decrease.

The obtained multiscale results suggest the possibility of tuning the thermal conductivity of graphene through fabrication of polycrystalline structures. It is worth mentioning that a recent experimental study[32] also proposed the fabrication of polycrystalline graphene structures for tailoring the electrical properties of graphene. This way, the main challenge is to accurately control the CVD process in order to reach the desired grain size for polycrystalline samples. Currently, this could be achieved by controlling the reactant flow rates, local environments and substrate properties in the CVD approach.[32,35,36] It has been widely reported that the CVD approach can produce polycrystalline structures with a grain size of 1 μm.[32–36] From an experimental point of view, the main efforts have been mainly devoted to increasing the grain size in order to reach single crystalline samples rather than fabrication of ultra-fine grained structures. However, fabrication of polycrystalline graphene structures with tunable thermal conductivity and corresponding electronic properties could be considered as an effective route for high efficiency 2D carbon-based thermoelectrics.

5. Conclusion

We proposed a combined atomistic and continuum multiscale approach to systematically study the effective thermal conductivity of polycrystalline graphene sheets. We performed MD simulations for the evaluation of the effective thermal conductivity of ultra-fine grained graphene sheets. The MD results reveal that the ultra-fine grained graphene structures have thermal conductivity one order of magnitude lower than that for pristine graphene. In addition, we constructed the continuum models of polycrystalline graphene samples using the finite element approach. In our finite element modeling, we assumed that all grain boundaries exhibit an effective thermal contact conductance. This effective thermal conductance was acquired by fitting the finite element results to the MD results for ultra-fine grained structures. By performing the finite element calculations for a wide range of grain sizes, close agreement between the finite element results and MD extrapolated results was observed. We found that for the ultra-fine grained graphene

Fig. 9 Line conductors in series with equal lengths connected with point conductors.

structures, the grain boundary contact resistance presents the major contribution toward the effective thermal resistance of the sample. We also found that the grain size distribution has a negligible effect on the thermal conductivity of polycrystalline graphene sheets for the grain sizes larger than 200 nm. Nevertheless, we found that by decreasing the grain size, the polycrystalline structures with non-uniform grain distributions have higher thermal conductivity than samples with uniform grain configurations. The proposed multiscale approach in this study could be considered as an efficient approach for the modeling of the thermal conductivity of polycrystalline graphene and other 2D structures such as boron-nitride and molybdenum disulfide sheets. The dependency of the graphene thermal conductivity on the grain size suggests that the controlled fabrication of polycrystalline graphene structures could be considered as an effective way for tuning the graphene thermal conductivity.

Appendix A

In this study, we extrapolate the EMD results for ultra-fine grained polycrystalline graphene by using a first order rational curve. This could be explained by studying the effective conductivity of a series of 'n' line conductors with equal length of L, connected with point conductors (as shown in Fig. 9). In this approach, line conductors and point conductors could be considered as grains and grain boundaries, respectively.

For this system, by assuming constant values for grain thermal conductivity (k_{grain}) and grain boundary conductance (k_{GB}), the effective conductivity, k_{eff}, is expressed by the following relationship:

$$\frac{n \times L}{k_{\mathrm{eff}}} = \frac{n \times L}{k_{\mathrm{grain}}} + \frac{(n-1)}{k_{\mathrm{GB}}}$$

This can be rewritten as follows:

$$k_{\mathrm{eff}} = \frac{n \times k_{\mathrm{grain}} \times k_{\mathrm{GB}} \times L}{(n-1)k_{\mathrm{grain}} + n \times k_{\mathrm{GB}} \times L}$$

This sample shows that the effective conductivity is dependent on the grain's length through a first order rational curve.

Acknowledgements

This work is partially funded by the European Union (ERDF) and the Free State of Saxony *via* TP A2 ("MolFunc"/"MolDiagnosik") of the Cluster of Excellence "European Center for Emerging Materials and Processes Dresden" (ECEMP). The Saxon State Ministry of Science and Arts and the Center for Advancing Electronics Dresden are acknowledged for their financial support. The Center for Information Services and High Performance Computing (ZIH) at TU Dresden is also acknowledged for providing the computational resources. The authors greatly appreciate Quirina Roode-Gutzmer for critical reading of the manuscript. VMD software[37] is used for graphical presentation of polycrystalline structures.

References

1 K. S. Novoselov, A. K. Geim, S. V. Morozov, D. Jiang, Y. Zhang, S. V. Dubonos, *et al.*, Electric field effect in atomically thin carbon films, *Science*, 2004, **306**, 666–669.
2 K. S. Novoselov, D. Jiang, F. Schedin, T. J. Booth, V. V. Khotkevich, S. V. Morozov, *et al.*, Two-dimensional atomic crystals, *Proc. Natl. Acad. Sci.*, 2005, **102**, 10451–10453.
3 Y. B. Zhang, Y. W. Tan, H. L. Stormer and P. Kim, Experimental observation of quantum Hall effect and Berry's phase in graphene, *Nature*, 2005, **438**, 201–204.
4 A. K. Geim and K. S. Novoselov, The rise of graphene, *Nat. Mater.*, 2007, **6**, 183–191.
5 S. Ghosh, W. Bao, D. L. Nika, S. Subrina, E. P. Pokatilov, C. N. Lau, *et al.*, Dimensional crossover of thermal transport in few-layer graphene, *Nat. Mater.*, 2010, **9**, 555–558.
6 C. Lee, X. Wei, J. W. Kysar and J. Hone, Measurement of the elastic properties and intrinsic strength of monolayer graphene, *Science*, 2008, **321**, 385–388.
7 J. R. Williams, L. DiCarlo and C. M. Marcus, Quantum Hall effect in a gate-controlled pn junction of graphene, *Science*, 2007, **317**, 638–641.
8 F. Banhart, J. Kotakoski and A. V. Krasheninnikov, Structural defects in graphene, *ACS Nano*, 2011, **5**, 26–41.
9 A. Reina, X. Jia, J. Ho, D. Nezich, H. Son, V. Bulovic, M. S. Dresselhaus and J. Kong, Large area, few-layer graphene films on arbitrary substrates by chemical vapor deposition, *Nano Lett.*, 2009, **9**, 30–35.
10 Z. Song, V. I. Artyukhov, B. I. Yakobson and Z. Xu, Pseudo Hall–Petch strength reduction in polycrystalline graphene, *Nano Lett.*, 2013, **13**, 1829–1833.
11 S. Malola, H. Hakkinen and P. Koskinen, Structural, chemical, and dynamical trends in graphene grain boundaries, *Phys. Rev. B: Condens. Matter*, 2010, **81**, 165447.
12 Y. Liu and B. I. Yakobson, Cones, pringles, and grain boundary landscapes in graphene topology, *Nano Lett.*, 2010, **10**, 2178–2183.
13 A. Bagri, S. P. Kim, R. S. Ruoff and V. B. Shenoy, Thermal transport across twin grain boundaries in polycrystalline graphene from nonequilibrium molecular dynamics simulations, *Nano Lett.*, 2011, **11**, 3917.
14 H. Y. Cao, H. Xiang and X. G. Gong, Unexpected large thermal rectification in asymmetric grain boundary of graphene, *Solid State Commun.*, 2012, **152**, 1807–1810.
15 J. Kotakoski and J. C. Meyer, Mechanical properties of polycrystalline graphene based on a realistic atomistic model, *Phys. Rev. B: Condens. Matter*, 2012, **85**, 195447.
16 D. V. Tuan, J. Kotakoski, T. Louvet, F. Ortmann, J. C. Meyer and S. Roche, Scaling properties of charge transport in polycrystalline graphene, *Nano Lett.*, 2012, **13**, 1730–1735.

17 S. Plimpton, Fast parallel algorithms for short-range molecular dynamics, *J. Comp. Physiol.*, 1995, **117**, 1–19.
18 D. W. Brenner, O. A. Shenderova, J. A. Harrison, S. J. Stuart, B. Ni and S. B. Sinnott, A second-generation reactive empirical bond order (REBO) potential energy expression for hydrocarbons, *J. Phys.: Condens. Matter*, 2002, **14**, 783–802.
19 J. Thomas, R. Iutzi and A. Mcgaughey, Thermal conductivity and phonon transport in empty and water-filled carbon nanotubes, *Phys. Rev. B: Condens. Matter*, 2010, **81**, 45413.
20 S. K. Chien, Y. T. Yang and C. K. Chen, Influence of hydrogen functionalization on thermal conductivity of graphene: Nonequilibrium molecular dynamics simulations, *Appl. Phys. Lett.*, 2011, **98**, 033107.
21 J. Hu, X. Ruan and Y. P. Chen, Thermal conductivity and thermal rectification in graphene nanoribbons: a molecular dynamics study, *Nano Lett.*, 2009, **9**, 2730–2735.
22 J. Hu, S. Schiffli, A. Vallabhaneni, X. Ruan and Y. P. Chen, Tuning the thermal conductivity of graphene nanoribbons by edge passivation and isotope engineering: A molecular dynamics study, *Appl. Phys. Lett.*, 2010, **97**, 133107.
23 J. Hu, W. Park, X. Ruan and Y. P. Chen, Thermal Transport in Graphene and Graphene-based Composites, *ECS Trans.*, 2013, **53**, 41–50.
24 L. Lindsay and D. A. Broido, Optimized Tersoff and Brenner empirical potential parameters for lattice dynamics and phonon thermal transport in carbon nanotubes and graphene, *Phys. Rev. B: Condens. Matter*, 2010, **82**, 205441.
25 B. Mortazavi, A. Rajabpour, S. Ahzi, Y. Rémond and S. M. Vaez Allaei, Nitrogen doping and curvature effects on thermal conductivity of graphene: A non-equilibrium molecular dynamics study, *Solid State Commun.*, 2012, **152**, 261–264.
26 B. Mortazavi and S. Ahzi, Molecular dynamics study on the thermal conductivity and mechanical properties of boron doped graphene, *Solid State Commun.*, 2012, **152**, 1503–1507.
27 L. F. C. Pereira and D. Donadio, Divergence of the thermal conductivity in uniaxially strained graphene, *Phys. Rev. B: Condens. Matter*, 2013, **87**, 125424.
28 J. Tersoff, New empirical approach for the structure and energy of covalent systems, *Phys. Rev. B: Condens. Matter*, 1988, **37**, 6991–7000.
29 J. Tersoff, Empirical interatomic potential for carbon, with applications to amorphous carbon, *Phys. Rev. Lett.*, 1988, **61**, 2879–2882.
30 E. Pop, V. Varshney and A. K. Roy, Thermal properties of graphene: Fundamentals and applications, *MRS Bull.*, 2012, **37**, 1273–1281.
31 B. Mortazavi, O. Benzerara, H. Meyer, J. Bardon and S. Ahzi, Combined molecular dynamics-finite element multiscale modeling of thermal conduction in graphene epoxy nanocomposites, *Carbon*, 2013, **60**, 356–365.
32 A. W. Tsen, L. Brown, M. P. Levendorf, F. Ghahari, P. Y. Huang, R. W. Havener, *et al.*, Tailoring electrical transport across grain boundaries in polycrystalline graphene, *Science*, 2012, **336**, 1143–1146.
33 G. W. Lee, R. C. Cooper, S. J. An, S. Lee, A. M. van der Zande, N. Petrone, A. G. Hammerberg, *et al.*, High-strength chemical-vapor-deposited graphene and grain boundaries, *Science*, 2013, **340**, 1073–1076.
34 P. Y. Huang, C. S. Ruiz-Vargas, A. M. van der Zande, W. S. Whitney, M. P. Levendorf, J. W. Kevek, *et al.*, Grains and grain boundaries in single-layer graphene atomic patchwork quilts, *Nature*, 2011, **469**, 389–392.
35 Y. Zhang, L. Zhang and C. Zhou, Review of Chemical Vapor Deposition of Graphene and Related Applications, *Acc. Chem. Res.*, 2013, **46**, 2329–2339.
36 A. Reina, X. Jia, J. Ho, D. Nezich, H. Son, V. Bulovic, M. S. Dresselhaus and J. Kong, Large area, few-layer graphene films on arbitrary substrates by chemical vapor deposition, *Nano Lett.*, 2009, **9**, 30–35.
37 W. Humphrey, A. Dalke and K. Schulten, VMD – Visual Molecular Dynamics, *J. Mol. Graphics*, 1996, **14**, 33–38.

